Tsukuba Geoenvironmental Sciences, Vol. 7, pp. 3-12, Dec. 26, 2011

Differences of synoptic fields depending on the location of MCS genesis in southwest China

Long XIE and Kenichi UENO*

Abstract

The locations of initiating Mesoscale Convective Systems (MCSs) in southwest (SW) China were examined using the Chinese geosynchronous satellite of China, and differences in synoptic-scale conditions were analyzed with Japanese objective analysis data. MCSs tended to occur along western mountainous margins in the evening, and those in the central Sichuan Basin occurred in after midnight. Four areas of intensive occurrences were identified in the Sichuan Basin, where a northern and a southeastern area overlapped with Mianyang and Chongquin City recording heavy rains accompanying severe disasters. Composite analysis of the synoptic fields revealed that MCS genesis in the southeastern area of Sichuan Basin was accompanied with the most eastward extension of a Tibetan High with a small ridge and rich-θe area on the eastern plateau areas. Case studies of heavy precipitation events showed that northern MCSs were born in the eastern edge of a convergence zone on the plateau with the development of mid-troposphere high-pressure areas in the east of SW China and southern MCSs were accompanied with the development of a short-wave transient trough with southwesterly rich moisture intrusion over the Sichuan Basin. Those characteristics suggested that thermally induced land-atmosphere interaction over the eastern TP is more important to initiate northwestern MCSs and the development of a short-wave trough in the leeward of a TP is more important for southern MCS genesis around the Sichuan Basin.

Key words: mesoscale convective system, heavy rain, southwest China

1. Introduction

Heavy precipitation events are frequently reported in SW China, in the upper reaches of the Yangtze River, during June and July. The SW area, located around 100°E - 110°E, 25°N - 35°N, consists of Sichuan, Guizhou, and Yunnan provinces and includes complex topography, such as the Sichuan Basin, the Yun-qui Plateau, and the Qinling Mountains in the leeward of the TP. Westerly flows are dynamically distorted, and thermally induced local circulations prevail there. The formation processes of a precipitation system and precipitation intensity/amount are closely affected by the thermo-dynamic functions of the complex topography. However, the mechanisms of severe convections have not been fully investigated from the viewpoint of geographical location and topographic effects. Moreover, many meteorological analyses have failed to investigate the relationships between the location of disturbances and actual heavy rain events that caused disasters.

General circulation in the monsoon season over the SW area is characterized as a confluence between the mid-latitude flows under a sub-tropical jet stream and a southwestern monsoon that forms leeward convergence and a shear zone (Tao and Ding, 1981). The moist southwestern monsoon passing along or over the Yun-qui Plateau provides low-level convective instability as a key factor to initiate a severe precipitation system (Li *et al*., 2007). The development of a small-scale cyclonic disturbance is well known as a southwest (SW) vortex or a Sichuan low (Tao and Ding, 1981), and mesoscale convective systems (MCSs) play an important diabatic role in systematizing intensive precipitation areas (Kuo *et al*., 1986). From the synoptic point of view, a mobile short-wave trough in the mid-latitude westerlies had been indicated to be an important factor for MCS eruption (Ma and Bosart, 1987). Fujinami and Yasunari (2009) detected two anomalous patterns propagating along the Asian jet around TP to affect the submonthly time-scale convective variability over the Yangtze River Basin. At the same time, the diurnal mode in precipitation records frequently shows a near-midnight maximum in the upper areas of the Yangtze River valley (Zhou *et al*., 2008). Several studies explain the diurnal mode in the evolution of meso-scale disturbances with different mechanisms, such as the propagation of mesoscale disturbances from the TP (e.g. Wang, 1987), the effects of land surface heating contrasts (e.g. Yamada *et al*., 2007), and diurnal monsoon variability (Chen *et al*., 2009). Recently, Ueno *et al*. (2011) found that the MCS in the southern part of Sichuan Basin was initiated with a sudden onset of local northerly winds after sunset under strong low-level wind shear between the southwesterly monsoon and northwesterly following a mid-latitude trough. Therefore, the diurnal development of MCSs in relation to synoptic fields that cause different topography

* Corresponding author: Kenichi Ueno, kenueno@sakura.cc.tsukuba.ac.jp

effects requires careful examination.

Although previous studies have suggested several factors involved in MCS formation, the dominant synoptic pattern that may affect the geographical location of MCS genesis has not been fully examined in the leeward region of the TP, especially around Sichuan Basin, where the population is large. Many heavy precipitation events have been analyzed as case studies in different areas, but few studies have compared the factors taking into account the location of the events. This study aimed first to clarify the distribution and diurnal variability of MCS occurrences and their relations to the in-situ records of heavy rain events in the SW area. The second aim was to characterize the synoptic pattern and formation mechanisms from the viewpoint of the prevailing MCS formation areas.

2. Occurrence of MCS and heavy rains

The occurrences of MCSs were automatically identified using the hourly infrared (IR) data from the Feng Yun 2 (FY2) spin-stabilized geosynchronous meteorological satellite of China provided by the Center for Environmental Remote Sensing, Chiba University. The FY2 satellite is located over the 105E longitude crossing the WS areas. The spatial resolution is 5 km at the nadir, which is suitable to detect the activity of severe convections in the target area. MCS identification was based on the methods of Evans and Shemo (1996) and applied in a domain of 100°E-110°E, 25°N-35°N to define the location and time of MCS genesis. According to these methods, an MCS is identified as a continuous area larger than 4000 km2 with Tbb lower than 219 K. If grids with Tbb lower than 235 K existed around the target cloud area, the grids were treated as candidate areas of MCS. More details regarding these methods are given in Sugimoto and Ueno (2010). The analysis period is June, July, and August (JJA) from 2008 to 2010. The sun-synchronized local time (LT) at 105E is seven hours ahead of the Coordinated Universal Time (UTC) and one hour behind Beijing Standard Time (BST).

In the SW area, monthly frequency of MCS occurrence showed a maximum in July with large year-to-year variability for three years. For example, the frequency in July 2010 was almost twice that in July 2008. One of the significant characteristics in the record of MCS occurrences is diurnal variability. Figure 1 shows the diurnal variation of hourly frequency in the MCS occurrences counted in a domain 100°-110°E, 25°-35°N. Most MCSs generated after noon through the night with three peaks, e.g., in the evening (at around 18 BST), before midnight (at around 21 BST), and after midnight (from 2 to 4 BST). The prevalence of a nocturnal precipitation system was consistent with the results based on gauge records in the east periphery of the TP (Yu *et al*., 2007). The location of MCS occurrence for the three time zones and their composition are plotted in Fig. 2. In the evening, e.g., 14-18 BST, MCSs tended to occur over western mountainous areas and along the eastern edge of the Yun-qui Plateau. Before midnight (from 20 to 23 BST), they occurred in the northwestern and southwestern portions of the Sichuan Basin. After midnight (from 2 to 6 BST), the distribution concentrated in the central basin area. Namely, early MCS onset tended to occur over western higher elevations, and nocturnal cases occurred over lower elevations. MCS genesis and its location are expected to be strongly linked to the diurnal modes of local circulation, which are controlled by the topography around the Sichuan Basin. In the composite map of all MCS occurrences (Fig. 2, lower right), four prevailing areas were defined around the Sichuan Basin, namely: A, northwestern portion near Mianyang City; B, western part near Ya'an City; C, southern part near Chongqin City; and D, southeastern periphery of the Yun-qui Plateau. In the next section, the mechanisms of MCS generation are examined on the basis of the four target areas.

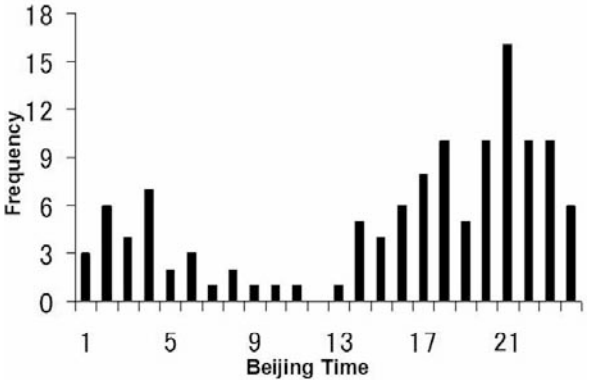

Fig. 1 Diurnal variation of MCS occurrence for 2008-2010 in southwest China.

Heavy rain events were extracted from the monthly reports of China Climate Events and Impacts (CCEI), Sichuan Climate Events and Impacts (SCEI), and electronic news from the news agency of Tencent (NT). The periods of event extraction are the same as those for MCS detection, and 29 events were extracted. The monthly reports and electric news focus mainly on heavy rain events with accompanying disasters. Therefore, cases involving heavy rain without an accompanying disaster were excluded from the comparison. From each event, the location and time of occurrence were identified. Fifteen cases of heavy rain occurred in July, and 23 cases occurred from 14 BST to 6 BST. These tendencies corresponded well with those of MCS occurrences shown in Fig. 1. The locations of heavy rain events with accompa-

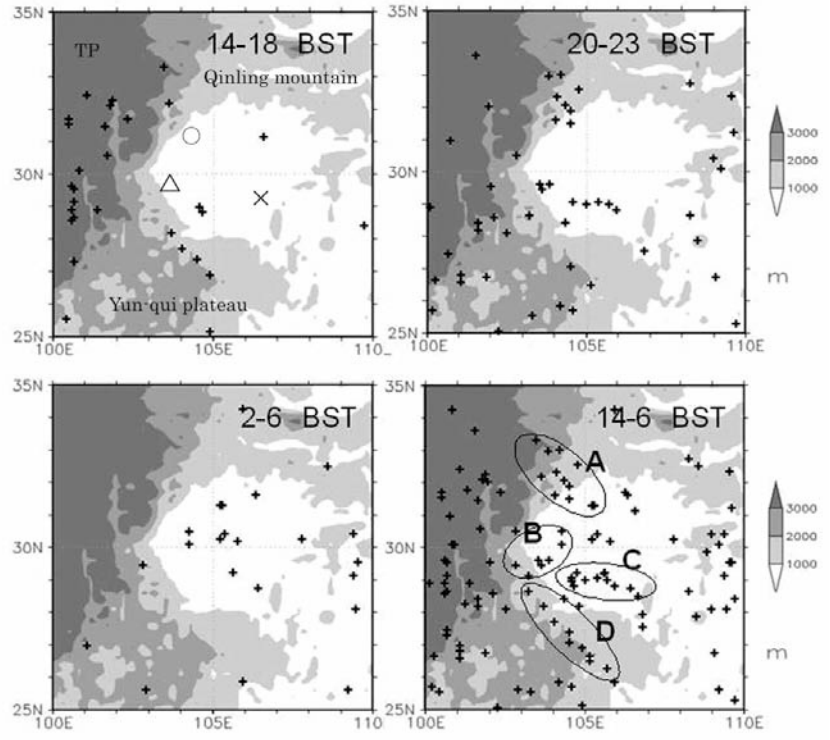

Fig. 2 Distribution of MCS genesis at 14-18 BST, 20-23 BST, 2-6 BST, and their total (14-6 BST) with intensive occurrence areas (A to D). City locations are identified as ○, Mianyang; ×, Chongqion; and △, Ya'an.

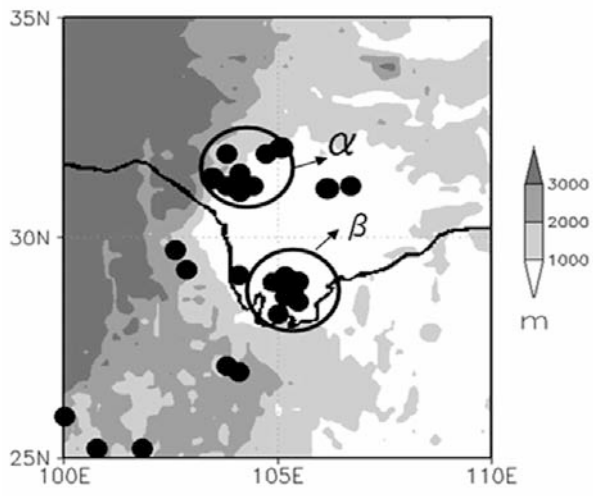

Fig. 3 Distribution of heavy rain events from 14 BST to 6 BST. The two intensive occurrence areas are identified as α and β.

nying disasters from 14 BST to 6 BST are plotted in Fig. 3. Two distinctive areas in northwestern and southern portions of Sichuan Basin, marked α and β, overlap with intensive MCS generated areas A and C in Fig. 2 (from 14 to 6 BST), respectively. These are also closed to the urbanized and populated areas of Mianyang and Chongqin City. Many of the disaster events in areas α and β were recorded during 19-22 BST and agreed with the MCS occurrences as mapped in Fig. 2 (upper right). On the other hand, reports of heavy rain with accompanying disasters are fewer in the intensive MCS-generation areas B and D. We speculated that such infrequent disasters despite the frequent occurrence of MCSs were due to the less dense population near the mountainous areas. In other words, nocturnal MCS genesis over areas A and C have more potential to impact humans and required further attention for weather nowcast and prediction.

3. Differences in synoptic scale environments

The characteristics of synoptic-scale circulations depending on the four different areas of intensive MCS occurrences defined in Fig. 2 are examined by composing upper and mid-troposphere pressure patterns and low-level wind and temperature fields. Figure 4 shows the composite maps of geopotential height with a wind vector at 200 hPa (left column) and geopotential height with equivalent potential temperature (θe) at 500 hPa (middle column) and a wind vector with θe at 850 hPa (right column). The uppermost figures show the climatological mean for June, July, and August (JJA) for three years (from 2008 to

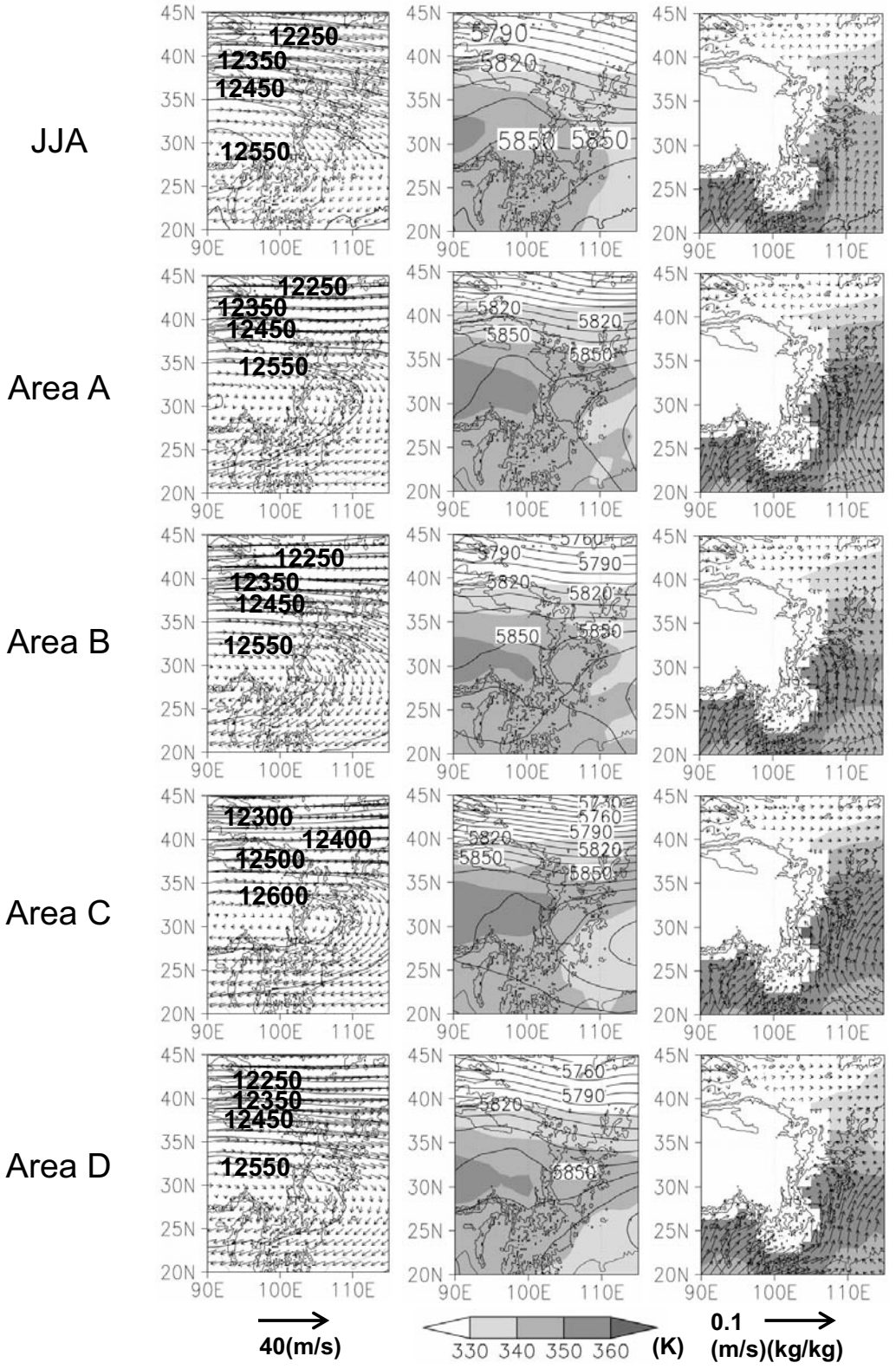

Fig. 4 JJA-averaged climate condition (upper most figures) and composite maps of synoptic-scale circulations with MCS occurrences in areas A to D, showing geopotential height with horizontal wind vector at 200 hPa (left column), geopotential height with θe at 500 hPa (middle column), and horizontal moisture flux (q*V) vector with θe at 850 hPa (right column).

2010), and the following figures are composites of cases of days of MCS occurrence for areas A to D, respectively. The composed number is 12 days for area A, 9 for area B, 13 for area C, and 9 for area D.

In the JJA mean, a center of upper high pressure (Tibetan anticyclone) locates over the southern TP, and westerlies prevail over the northern plateau. At mid-troposphere, weak westerly flows intrude over the SW area from the TP areas. The southwest monsoon with high θe extends in the south of the Sichuan Basin at 850 hPa. In the cases of MCS genesis, a Tibetan anticyclone extended eastward, indicating that upper high pressure areas were intensified by the adiabatic heating of MCS developments. At 500 hPa, westerlies over the TP were weakened, and a shortwave trough was recognized in the north of 33N along the northwestern periphery of the plateau (at 102.5E). The extension of the Tibetan anticyclone was more evident for the cases in area C, with an apparent high θe zone spreading over eastern TP and a high pressure center in the east of SW China at 500 hPa. The feature suggests that MCS events over the southern portion of Sichuan Basin (area C) have more potential to heat up the middle and upper troposphere after the onset.

For all cases, a low-level southwest monsoon intruded north of the Sichuan Basin at 850 hPa, and southeasterly ascending flows with a convergence line existed over the MCS-generation area. However, a mid-troposphere shortwave pattern along the eastern periphery of TP slightly differed depending on the location of MCS genesis. The wave, such as a small ridge at 98E and a trough at 102E at around 33N at 500 hPa, was not clear in the cases of area B. For the MCS genesis cases in areas A and C, the longitudinal pressure gradient in the west of the ridge increased and provided favorable conditions for the intrusion of a southwesterly monsoon into the central TP to increase the θe. When the MCS occurred in the southernmost area D, weak west-northwestern dry flows prevailed over the northwestern TP without a high θe over the eastern TP. At 850 hPa, the main southwest monsoon channel was limited in the south of Sichuan Basin, with small cyclonic convergence flows over the target area. Namely, the MCS genesis in each location was associated with the modification of shortwave patterns that accompanied different near-surface flow pattern and instability over the eastern TP.

4. Case studies

Four heavy precipitation events occurred in areas A-D are nominated respectively, and actual synoptic condition that erupted an MCS are examined. Facts of precipitation records with disaster conditions are summarized in Table 1. The cloud distribution and circulation of mid- and lower-tropospheres are shown in Figs. 5 and 6. Figure 6 contains snapshots when the target MCS almost maximized its area, and the images in Fig. 5 correspond to six hours prior to those in Fig. 6. In all cases, MCSs kept their locations during the developing and decaying stages, and the stationary movement caused intensive precipitation in the same areas. The first case covers July 14-16, when the MCS occurred in area A. According to SCEI, the total precipitation amount was more than 200 mm in Mianyang City, and nine people died. After 16 BST on July 14, multiple cloud clusters developed along a convergence zone on the TP and then moved eastward and systematized into a single zonal mesoscale system. A target MCS was born in the east of the TP (around 104E33N) at 5 BST, maximized the area at 10 BST, and extinguished at 19 BST in almost the same location. The second case occurred on Aug. 18-19 in area B. According to NT, the accumulated precipitation in 12 hours was 195.5 mm in Ya'an, and more than 6,000 houses were destroyed. Zonal cloud activities started after 17 BST on Aug. 18 in the eastern TP, and an isolated cloud area was then initiated at 21 BST at the location of 105E30N, which developed into an MCS at the same location. The MCS maximized the area at 4 BST on Aug. 19 and diminished at 15 BST. The two cases presented above indicate that an MCS developed on the eastern edge of a convergence zone formed over the plateau. A third case occurred on Aug. 3 and provided more than 400 mm of total precipitation in area C. Two MCSs were initiated after 18 BST at 101E29N and 106E27N. They then merged into a zonal system at 2 BST on Aug. 4 and maintained the location until 6 BST. For the fourth case on July 26, the total precipitation amount was relatively less than that in other cases. In the beginning, several cloud clusters were initiated over the south-

Table 1 Facts of four heavy rain events

	Period	Place (City)	Precipitation amount	Damages	Source
Case 1	July 14-16	Mianyang	200 mm/ total	Lost 9 persons	SCEI
Case 2	Aug. 18-19	Yaan	195.5mm/ 12 hours	Lost houses etc.	NT
Case 3	Aug. 3-4	Chongqin	412.6 mm/ total	Lost houses etc.	NT
Case 4	July 26-27	Chongqin	153 mm/ 13 hours	Lost 22 persons	SCEI

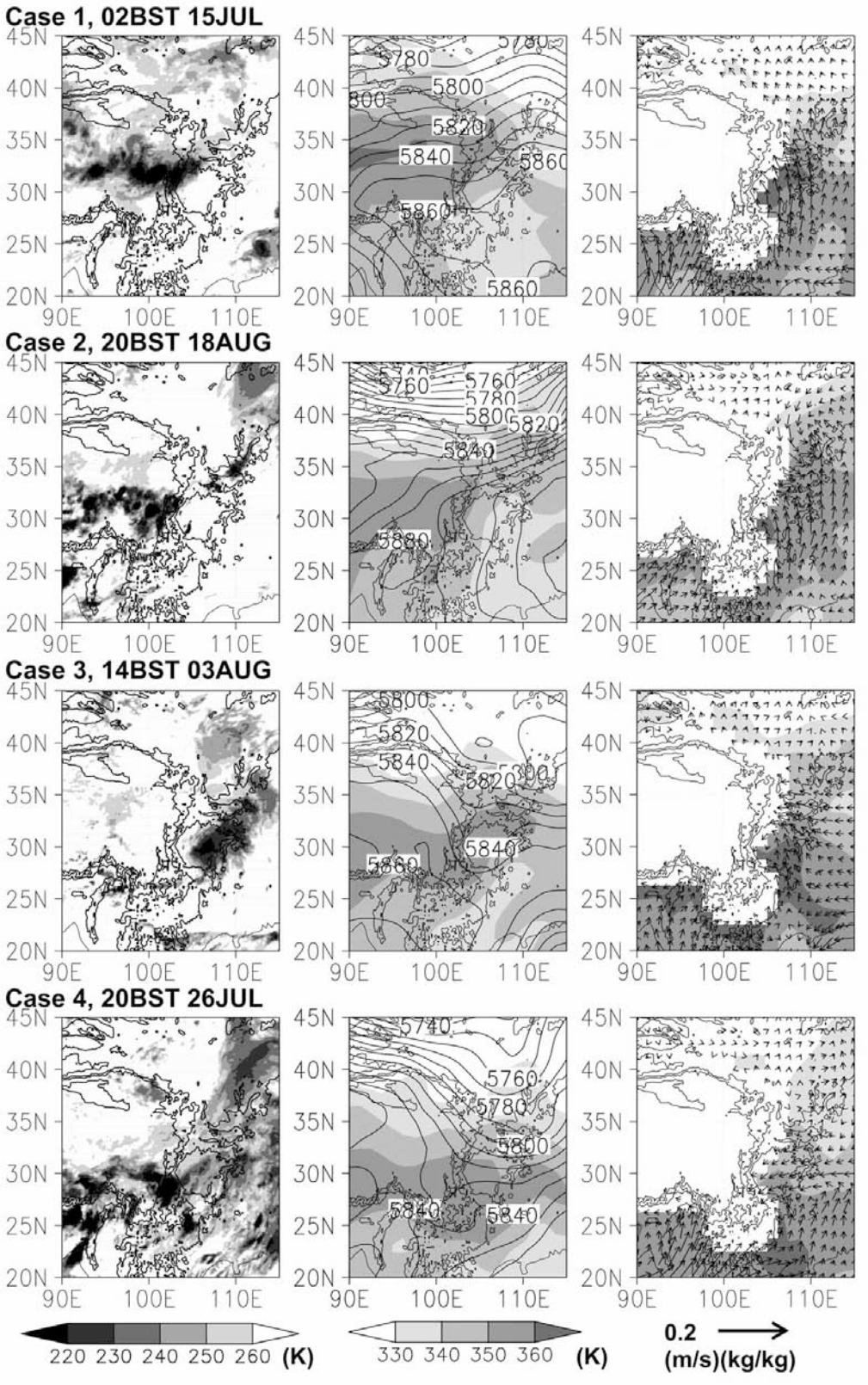

Fig. 5 Cloud distribution and synoptic-scale circulations for Case 1 at 2 BST, July 15, Case 2 at 20 BST, Aug. 18, Case 3 at 14 BST, Aug. 3, and Case 4 at 20 BST, July 26. The FY2 Tbb distribution (left), geopotential height with θe at 500 hPa, and horizontal moisture flux vector with θe at 850 hPa (right) are shown.

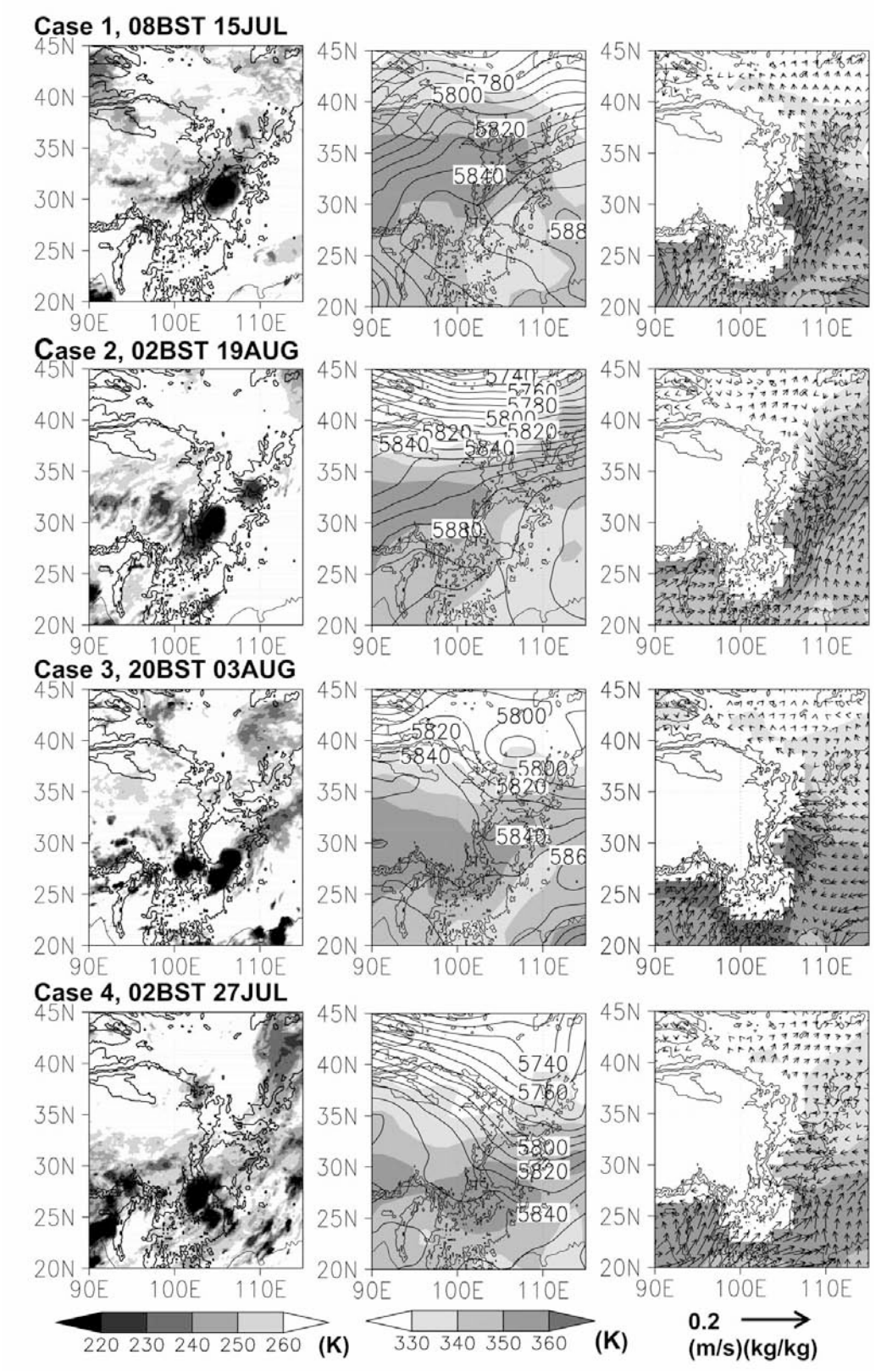

Fig. 6 Same as Fig. 5, but for the scenes six hours later.

eastern periphery of the TP (around 20N102E) at around 17 BST. We speculate that they were thermally induced diurnal convections over the Himalayas. At the same time, a single cell was born at 105E25N and developed into a mesoscale system. A former cloud cluster migrated eastward and merged with the latter system to develop a large MCS at 4 BST on July 27 that induced disasters in area D. For Cases 3 and 4, precipitation systems had not migrated from the plateau areas, but they originated and strengthened separately from the plateau or coupled and then strengthened. Especially, the results from Case 3 were quite similar to those obtained by Ueno *et al*. (2011).

The progress of convective activity captured by Tbb images with circulations in the middle troposphere was different between Cases 1 and 2 and Cases 3 and 4. In Cases 1 and 2, a zonal cloud band was initiated on the eastern central plateau at first and systematized in the afternoon (left columns in Fig. 5). In the 500 hPa, high-pressure areas extended in the mid-troposphere from the southeast over the SW China, causing a latitudinal pressure gradient over the central plateau with a convergence zone between monsoon flows and mid-latitude air mass (Fig. 5, center). The cloud zone over the eastern TP was associated with wind convergence and increases of θe near the plateau surface. The MCS originated on the eastern edge of the cloud zone and developed over the northwestern or western Sichuan Basin with a low-level southeasterly monsoon. A low-level rich-θe zone appeared along the eastern slopes of the TP before the MCS formation, providing convective instability (Fig. 5 right), and dissolved after the formation. The formation process of MCSs in the leeward of the TP accompanied with a convergence line over the plateau was similar to the results by Yasunari and Miwa (2006), who proposed the Plateau Edge Cyclogenesis mechanism.

In Cases 3 and 4, MCSs generated away from the plateau without the apparent formation of cloud zones on the plateau. Convections along the southern periphery of the plateau in Case 4 (shown in Fig. 5, lower-left) were orographically induced clouds along the Himalayas and different from the convergence-type one, as shown in Cases 1 and 2. Moreover, a shortwave trough extended southward at 500 hPa along the eastern periphery of the plateau into which northwesterly drier flows intruded from mid-latitudes over the northeastern TP (middle columns in Fig. 5). At that moment, high-pressure areas in the southeast, as shown in Cases 1 and 2, were not recognized. Low-level easterly dry intrusion is more evident over the northern basin, with a prominent cyclonic vortex between the southwesterly monsoon and mid-latitude easterly. A rich θe zone extended over the Sichuan Basin at 500 hPa. The results from Case 3 closely resembled those obtained by Ueno *et al*. (2011), which revealed the importance of northwesterly flows following a mid-latitude trough that was captured by the Sichuan Basin and caused a sudden onset of MCSs under conditions of a rich θe day over area C. Accordingly, a case study for heavy rain events suggested that MCSs formed on the northwestern or western portion of the Sichuan Basin tend to be oriented by the convergences with vortices over the eastern plateau under the synoptic conditions of extending high-pressure areas in the mid-troposphere from the western pacific side. On the contrary, the extension of the shortwave trough along the eastern plateau slope with rich θe intrusion along the southeastern plateau played an important role in the formation of MCSs in the southern basin or northeastern edge of the Yun-qui Plateau.

5. Summary and discussion

The occurrences of MCSs in southwest China were examined based on FY2-IR images and compared with heavy rain events with accompanying disasters for three years. The MCS genesis was concentrated in the evening (around 18 BST), night (around 21 BST), and after midnight (2-4 BST). Evening MCSs tended to originate over the western mountain sides, and midnight MCSs tended to originate in the Sichuan Basin. In the Sichuan Basin, four concentrated areas of MCS genesis were identified in the northwestern portion near Mianyang city, the western part near Ya'an, the southern part near Chongqin City, and the southeastern periphery of the Yun-qui plateau. Two of them showed good correspondence with the areas of frequent occurrence of heavy precipitation events with accompanying disasters. The results suggested that the combination of diurnal thermo-dynamic effects by the plateau surface and local topography play different roles depending on the areas of MCS initiation. In other words, a fine-mesh numerical simulation that could treat the diurnal changes of flow patterns around the eastern periphery of the TP is essential to diagnose MCS formations and predict heavy rains.

Composite analyses for synoptic scale circulations were conducted for the different locations of MCS genesis and compared with case studies of heavy precipitation events with accompanying disasters. The development of a small shortwave was recognized for the MCSs in areas A, C, and D. The composite of MCS genesis for the area southeastern of Sichuan Basin (area C) showed the most eastward extension of Tibetan High with a small ridge and rich-θe zone at the eastern plateau surface level. Case studies showed wind convergence zones distributing east-west with active convections over TP prior to the development of MCS in areas A and B. The development of a mid-troposphere high-pressure pattern over the Western

Pacific played an essential role in characterizing the synoptic-scale circulations. On the contrary, the composites for the areas south or southwest of Sichuan Basin (areas C and D) showed southward development of a shortwave trough along the eastern periphery of TP that induced northwestern intrusion from the mid-latitudes over the northeastern TP. A low-level cyclonic vortex was then strengthening southeast of the TP under rich θe air mass extending from the southeastern periphery of the plateau.

There was an inconsistent tendency between the composite analysis in Section 3 and the case studies in Section 4. The apparent shortwave trough analyzed in Cases 3 and 4 was not clearly analyzed in the composite map in Fig. 4. One of the reasons may be that the cases for Section 4 were selected on the basis of the news of heavy rain and the cases for the synoptic composite by the location of MCSs. Other problems are the differences between the stationery wave along the lee-side of the mountain, as shown in Fig. 4, and the transient shortwave, as shown in Fig. 5 and 6. The features of those waves also differ depending on the reanalysis data around the TP. We speculate that land-surface and atmosphere interactions over the eastern TP are more important for the origin of the MCSs in a plateau-scale convergence zone and affect heavy rain events in the area north or west of the Sheehan Basin. Furthermore, the dynamic function of plateau edge topography to propagate low-level flows along the eastern TP following the development of a shortwave trough is more important for the southern cases. One key issue is to reveal the structure of the development of a mid-troposphere shortwave coupled with diurnal local circulations. Further analysis needs to be conducted to verify the hypothesis together with mesoscale intensive observation data and multi-ensemble numerical simulations.

Acknowledgements

The work described in this publication has been supported by the European Commission (Call FP7-ENV-2007-1 Grant No. 212921) as part of the CEOP – AEGIS project (http://www.ceop-aegis.org/) coordinated by the Université Louis Pasteur. FY2 data was provided from the Center for Environmental Remote Sensing, Chiba University. The authors are grateful to Dr. S. Sugimoto of the University of Tsukuba, who helped produce the figures and provided valuable comments.

References

Chen, G., W. Sha, and T. Iwasaki, 2009: Diurnal variation of precipitation over southeastern China: Spatial distribution and its seasonality. *J. Geophys. Res.*, **114**, D13103, doi:10.1029/ 2008JD011103.

Evans, L. J., and R. E. Shemo, 1996: A procedure for automated satellite-based identification and climatology development of various classes of organized convection. *J. Appl. Meteorol.*, **35**, 638-652, doi:10.1175/1520-0450(1996)035<0638:APFASB>2.0.CO;2.

Fujinami, H., and T. Yasunari, 2009: The effects of mid-latitude wave over and around the Tibetan Plateau on submonthly variability of the East Asian summer monsoon. *Mon. Wea. Rev.*, **137**, 2286-2304.

Kuo, Y., L. Cheng, and R. Anthes, 1986: Mesoscale analysis of the Sichuan flood catastrophe, 11-15 July 1981. *Mon. Wea. Rev.*, **114**, 1984-2003.

Li, Z., T. Takeda, K. Tsuboki, K. Kato, M. Kawashima, and Y. Fujiyoshi, 2007: Nocturnal evolution of cloud clusters over eastern China during the intensive observation periods of GAME/HUBEX in 1998 and 1999. *J. Meteor. Soc. Japan*, **85**, 25-45.

Ma, K-Y., and L. F. Bosart, 1987: A synoptic overview of a heavy rain event in southern China. *Weather and Forecasting*, **2**, 89-112.

Sugimoto, S., and K. Ueno, 2010: Formation of mesoscale convective systems over the eastern Tibetan Plateau affected by plateau-scale heating contrasts. *J. Geophys. Res.*, **115**, D16105, doi:10.1029/2009JD013609.

Tao, S.-Y., and Y. H. Ding, 1981: Observational evidence of the influence of the Qinghai-Xizang (Tibet) Plateau on the occurrence of heavy rain and severe convective storms on China. *Bull. Amer. Meteor. Soc.*, **62**, 23-30.

Ueno, K., S. Sugimoto, T. Koike, H. Tsutsui, and X. Xu, 2011: Generation processes of mesoscale convective systems following mid-latitude troughs around the Sichuan Basin. *J. Geophys. Res.,* **115**, D16105, doi:10.1029/2009JD013609.

Wang, B., 1987: The development mechanism for Tibetan Plateau warm vortices. *J. Atmos. Sci.*, **44**, 2978-2994, doi:10.1175/1520-0469(1987) 044<2978: TDMFTP>2.0.CO;2.

Yamada, H., B. Geng, H. Uyeda, and K. Tsuboki, 2007: Thermodynamic impact of the heated landmass on the nocturnal evolution of a cloud cluster over a Meiyu/Baiu front. *J. Meteorol. Soc. Japan*., **85**, 663-685, doi:10.2151/jmsj.85.663.

Yasunari, T., and T. Miwa, 2006: Convective cloud systems over the Tibetan Plateau and their impact on mesoscale disturbances in the Meiyu/Baiu frontal zone -A case study in 1998 -. *J. Meteor. Soc. Japan*, **84**, 783-803.

Yu, R., T. Zhou, A. Xiong, Y. Zhu, and J. Li, 2007: Diurnal variation of summer precipitation over contiguous China. *Geophys. Res. Let.*, **34**, L01704, doi:10.1029/2006GL028129.

Zhou, T., R. Yu, H. Chen, A. Dai, and Y. Pan, 2008: Summer precipitation frequency, intensity, and diurnal cycle over China: A comparison of satellite data with rain gauge observations. *J. Clim.*, **21**, 3997-4010, doi:10.1175/2008JCLI2028.1.

Received 7 September 2011
Accepted 10 November 2011